

Magnetic circular dichroism of nonresonant x-ray Raman scattering

N. Hiraoka,^{1,*} M. Takahashi,² W. B. Wu,¹ C. H. Lai,¹ K. D. Tsuei,¹ and D. J. Huang¹

¹National Synchrotron Radiation Research Center, Hsinchu 30076, Taiwan

²Faculty of Engineering, Gunma University, Kiryu, Gunma 376, Japan

(Received 13 February 2015; revised manuscript received 25 May 2015; published 22 June 2015)

We report on the magnetic circular dichroism of nonresonant x-ray Raman scattering. The circular dichroism has been observed at the $L_{II,III}$ edges on a pure iron sample. The observed magnetic effect is $\sim 2\%$. The dichroism spectra exhibit a significant dependence on the direction of the magnetization vector. We have constructed an effective theory to understand these behaviors. The dichroism arises from the orbital scattering and the spin scattering having different angular dependences. The calculation reproduces well the observed spectra.

DOI: [10.1103/PhysRevB.91.241112](https://doi.org/10.1103/PhysRevB.91.241112)

PACS number(s): 78.70.Ck, 78.20.Bh, 78.20.Ls, 78.30.Er

Magnetic circular dichroism (MCD) and also linear dichroism (MLD) have been long studied in various types of spectroscopic techniques. The magneto-optical Kerr effect and the Faraday effect by visible or infrared light are well-known phenomena, discovered in the 19th century. On the other hand, the history of MCD/MLD studies by x rays is relatively short: After the theoretical study by Erskine and Stern in 1975 and the first observation by Schütz *et al.* in 1987 [1,2], studies rapidly progressed owing to advances in the synchrotron radiation sources in the 1980's–1990's [3–5]. Particularly, x-ray absorption spectroscopy (XAS)-MCD in the soft x-ray region, e.g., at the L edge in transition metals, has intensively been explored using sum rules to evaluate the magnitude of a spin and/or an orbital magnetic moment [6–8]. Today, XAS-MCD is a standard tool used to study the magnetic properties of materials. In addition, resonant/nonresonant magnetic scattering [9–11] and magnetic Compton scattering [12,13] are also types of dichroism. It is noted here that there are several reports investigating the MCD in *resonant* inelastic scattering or emission, too [14–16].

Nevertheless, reports of MCD in *nonresonant* inelastic x-ray scattering or x-ray Raman scattering (XRS) are lacking. This may be an unexpected fact because it is widely believed that XRS has a close similarity to XAS [17,18]. For example, the transition matrix of XRS becomes similar to that of XAS at small momentum, the so-called dipole approximation. Nowadays, an absorption edge in the soft x-ray region is often measured by XRS instead of XAS if the strong absorption of soft x rays is an issue, typically, in high-pressure studies [19–25]. There are two reasons why MCD has yet to be reported in XRS. First, the experiment is technically difficult. The scattering cross section of XRS is very small and thus it is difficult to obtain data with a high statistical accuracy. The second reason may be a more essential problem: It is unclear whether or not MCD is actually observable in XRS, as discussed below.

Using a perturbation Hamiltonian (H) for an interaction between photons and an electron, the transition matrix between the initial state $|I\rangle$ and the final state $|F\rangle$ is given as

$$\langle F|H|I\rangle = (\mathbf{e}_i \cdot \mathbf{e}_f) \langle f|e^{i\mathbf{Q}\cdot\mathbf{r}}|i\rangle. \quad (1)$$

Therefore, the double differential cross section or the intensity is simply given as

$$\left(\frac{d^2\sigma}{d\Omega d\omega}\right)_{\lambda_i \rightarrow \lambda_f} \propto \sum_f (\mathbf{e}_i \cdot \mathbf{e}_f)^2 |\langle f|e^{i\mathbf{Q}\cdot\mathbf{r}}|i\rangle|^2 \delta_\omega. \quad (2)$$

$\mathbf{Q} = \mathbf{q}_i - \mathbf{q}_f$ is the scattering vector and \mathbf{r} stands for the position of the electron. $|i\rangle$ ($|f\rangle$) represents the initial (final) state for the electron while $\mathbf{q}_{i(f)}$ and $\lambda_{i(f)}$ are the wave vector and the polarization state of the photons, respectively. δ_ω represents the energy conservation. The polarization term is simply given as $(\mathbf{e}_i \cdot \mathbf{e}_f)^2$, where $\mathbf{e}_{i(f)}$ is the photon polarization vector, but this term just leads to the prefactor in Thomson scattering, i.e., $(\mathbf{e}_i \cdot \mathbf{e}_f)^2 \rightarrow \frac{1}{2}(1 + \cos^2 \Theta + P_L \sin^2 \Theta)$ once λ_f is integrated. Here, Θ is the scattering angle. Equation (2) only depends on the linear polarization parameter P_L , rather than the circular polarization parameter P_C , and therefore it does not predict MCD. This is the main reason why it has been suspected if XRS-MCD is actually observable. The situation is in contrast to the resonant case, basically understood as a combination of two processes of x-ray absorption and subsequent x-ray emission (via an intermediate state), both of which often show MCD [14–16].

However, in a similar way to other nonresonant-type magnetic scatterings, higher-order terms such as relativistic perturbation may generate MCD. Such perturbation terms were already formulated by Blume in 1985 [26]. With the electron momentum \mathbf{p} and the spin \mathbf{s} ,

$$H = f_c + f_i + f_s, \quad (3a)$$

$$f_c = (\mathbf{e}_i \cdot \mathbf{e}_f) e^{i\mathbf{Q}\cdot\mathbf{r}}, \quad (3b)$$

$$f_i = g e^{i\mathbf{Q}\cdot\mathbf{r}} \frac{\mathbf{Q} \times \mathbf{p}}{\hbar q_i^2} \cdot \mathcal{A}, \quad (3c)$$

$$f_s = -ig e^{i\mathbf{Q}\cdot\mathbf{r}} \mathbf{s} \cdot \mathcal{B}, \quad (3d)$$

where

$$\mathcal{A} = \mathbf{e}_f \times \mathbf{e}_i, \quad (3e)$$

$$\mathcal{B} = \mathbf{e}_f \times \mathbf{e}_i + (\hat{\mathbf{q}}_f \times \mathbf{e}_f)(\hat{\mathbf{q}}_f \cdot \mathbf{e}_i) - (\hat{\mathbf{q}}_i \times \mathbf{e}_i)(\hat{\mathbf{q}}_i \cdot \mathbf{e}_f) - (\hat{\mathbf{q}}_f \times \mathbf{e}_f) \times (\hat{\mathbf{q}}_i \times \mathbf{e}_i). \quad (3f)$$

Here, $g = \hbar\omega m^{-1}c^{-2}$ is given by the photon energy $\hbar\omega$, divided by the electron rest energy mc^2 ($=0.511$ MeV with light velocity c and electron rest mass m), and determines the magnitude of the magnetic effect. It is noted that f_c arises from

*hiraoka@spring8.or.jp

the first-order perturbation while f_i arises from the second-order perturbation, and finally f_s is the sum of those involving relativistic effects. The elastic case was carefully examined by Blume and Gibbs in 1988 [27], and finally a remarkably simple formula was obtained by Collins *et al.* in 1992 [10]. Their formula becomes especially simple at $\Theta = 90^\circ$:

$$\begin{aligned} d\sigma/d\Omega &\propto |\langle f|H|i\rangle_{f\rightarrow i}|^2 \\ &\rightarrow n(\mathbf{Q})[(1 + P_L)n(\mathbf{Q}) \\ &\quad + 2gP_C\{\mathbf{S}(\mathbf{Q}) \cdot \hat{\mathbf{q}}_f + \frac{1}{2}\mathbf{L}(\mathbf{Q}) \cdot (\hat{\mathbf{q}}_f + \hat{\mathbf{q}}_i)\}]. \end{aligned} \quad (4)$$

Note that the P_L is defined here to be negative when the polarization is on the scattering plane. $n(\mathbf{Q})$ provides the electron form factor or the Fourier transform of the charge density while $\mathbf{S}(\mathbf{Q})$ and $\mathbf{L}(\mathbf{Q})$ provide those of the spin and the orbital magnetic moments, respectively. This formula explicitly includes P_C , and thus clearly contains the MCD effect.

We have carefully examined the scattering amplitudes Eqs. (3a)–(3f). They are still applicable to XRS and an effective formula is available as Eq. (4) after adopting several approximations and modifications. The most striking difference is the handling of the orbital part (3c). As indicated by Trammel [28,29], an additional dipolar (or multipolar) term exists when the $\mathbf{Q} \times \mathbf{p}$ term is converted into $\mathbf{L}(\mathbf{Q})$. In the following we limit our discussion below to the dipole transition. Under this approximation, Trammel's equation is rewritten as

$$\begin{aligned} e^{i\mathbf{Q}\cdot\mathbf{r}} \frac{a_0}{\hbar} \mathbf{p} &\rightarrow i \frac{\hbar\omega_i - \hbar\omega_f}{E_H} \frac{\mathbf{r}}{a_0} + \frac{(a_0Q)^2}{6} \\ &\times \left[\frac{\hat{\mathbf{Q}} \times \mathbf{L}}{\hbar} \left(\hat{\mathbf{Q}} \cdot \frac{\mathbf{r}}{a_0} \right) + \left(\hat{\mathbf{Q}} \cdot \frac{\mathbf{r}}{a_0} \right) \frac{\hat{\mathbf{Q}} \times \mathbf{L}}{\hbar} \right] \\ &+ \dots \end{aligned} \quad (5)$$

a_0 is the Bohr radius while \hbar is the Planck constant. The Hartree energy E_H is given as $me^4\hbar^{-1} = 27.21$ eV, with the electron charge e . The first term produces the dipolar transition and the magnitude is proportional to the energy difference of the initial and the final states. This becomes zero for elastic scattering or a very small contribution for low-energy excitations such as phonons or magnons. However, this term can have a significant contribution in XRS. In addition to the dipole approximation already mentioned, we adopt the specular scattering approximation, namely, $\hat{\mathbf{Q}}$ is assumed to be exactly centered between $\hat{\mathbf{q}}_i$ and $-\hat{\mathbf{q}}_f$. Then, $\hat{\mathbf{Q}} = \mathbf{Q}|\mathbf{q}_i - \mathbf{q}_f|^{-1} \rightarrow (\hat{\mathbf{q}}_i - \hat{\mathbf{q}}_f)|\hat{\mathbf{q}}_i - \hat{\mathbf{q}}_f|^{-1}$. This transformation allows us to obtain forms similar to Eqs. (3a)–(3f). We may rewrite the scattering amplitude as

$$H_1 = f_{C1} + f_{OE1} + f_{OM1} + f_{SM1}, \quad (6a)$$

$$f_{C1} = (i\mathbf{Q} \cdot \mathbf{r})(\mathbf{e}_i \cdot \mathbf{e}_f), \quad (6b)$$

$$f_{OE1} = -ig \frac{\beta - 1}{\alpha} \frac{(\mathbf{Q} \times \mathbf{r})}{a_0Q} \cdot \mathcal{A}', \quad (6c)$$

$$f_{OM1} = -\frac{i}{6}g\gamma \left\{ 2(i\mathbf{Q} \cdot \mathbf{r}) \frac{\mathbf{L}'}{\hbar} + (\mathbf{Q} \times \mathbf{r}) \right\} \cdot \mathcal{A}', \quad (6d)$$

$$f_{SM1} = -ig(i\mathbf{Q} \cdot \mathbf{r})(\mathbf{s} \cdot \mathcal{B}'), \quad (6e)$$

where

$$\mathcal{A}' = (\mathbf{e}_f \times \mathbf{e}_i)|\hat{\mathbf{q}}_i - \hat{\mathbf{q}}_f|, \quad (6f)$$

$$\begin{aligned} \mathcal{B}' &= \frac{1 + \beta}{2}(\mathbf{e}_f \times \mathbf{e}_i) + \beta(\hat{\mathbf{q}}_f \times \mathbf{e}_f)(\hat{\mathbf{q}}_f \cdot \mathbf{e}_i) - (\hat{\mathbf{q}}_i \times \mathbf{e}_i)(\hat{\mathbf{q}}_i \cdot \mathbf{e}_f) \\ &\quad - \frac{1 + \beta}{2}(\hat{\mathbf{q}}_f \times \mathbf{e}_f) \times (\hat{\mathbf{q}}_i \times \mathbf{e}_i), \end{aligned} \quad (6g)$$

$$\mathbf{L}' = \hat{\mathbf{Q}} \times (\hat{\mathbf{Q}} \times \mathbf{L}). \quad (6h)$$

Here, α is the fine-structure constant, given as $e^2c^{-1}\hbar^{-1} = 1/137.06$. We define $\beta = \omega_f/\omega_i$ as the ratio q_f/q_i and $\gamma = |\hat{\mathbf{q}}_i - \beta\hat{\mathbf{q}}_f|$ as Q/q_i . The details of the derivation will be described elsewhere (see the Supplemental Material [30]). f_{C1} arises from the first-order process while f_{OE1} and f_{OM1} arise from the second-order process. f_{SM1} involves the relativistic effect. The amplitude of f_{OE1} is as small as 5% of f_{C1} while those of f_{OM1} and f_{SM1} are $\sim 1\%$. The f_{OE1} arises from the first term in Eq. (5), having a simple form, while f_{OM1} from the second term has a complex form. The major part of the orbital scattering is f_{OE1} , having a five times larger amplitude than f_{OM1} in typical XRS-MCD experiments. In order to achieve a qualitative interpretation, we ignore the latter below: $f_{OM1} \rightarrow 0$. With a similar procedure as in Ref. [27], now we finally obtain a similar expression as Eq. (4) at $\Theta = 90^\circ$:

$$\begin{aligned} \frac{d^2\sigma}{d\Omega d\omega_f} &\rightarrow \sum_f \left[(1 + P_L)N_{\hat{\mathbf{n}}}^*N_{\hat{\mathbf{n}}} + 2gP_C \right. \\ &\quad \left. \times \text{Im} \left(\frac{\beta - 1}{\alpha} N_{\hat{\mathbf{n}}}O_{\hat{\mathbf{n}}}^* + \frac{\beta + 1}{2} N_{\hat{\mathbf{n}}}S_{\hat{\mathbf{n}}}^* \right) \right] \delta_\omega, \end{aligned} \quad (7a)$$

where

$$N_{\hat{\mathbf{n}}} = \langle f|(i\mathbf{Q} \cdot \mathbf{r})|i\rangle, \quad (7b)$$

$$O_{\hat{\mathbf{n}}} = \langle f|(i\hat{\mathbf{q}}_f \times \hat{\mathbf{q}}_i) \cdot (\mathbf{r}/a_0)|i\rangle, \quad (7c)$$

$$S_{\hat{\mathbf{n}}} = \langle f|(\mathbf{Q} \cdot \mathbf{r})(\mathbf{s} \cdot \hat{\mathbf{q}}_f)|i\rangle. \quad (7d)$$

The primary term is purely charge scattering (represented by $N_{\hat{\mathbf{n}}}$) while the second term results from the interference between the charge scattering and the orbital ($O_{\hat{\mathbf{n}}}$) or the spin scattering ($S_{\hat{\mathbf{n}}}$). The above formula explicitly includes P_C , and therefore MCD can be detected.

The experiment was performed at the Taiwan inelastic scattering beamline at SPring-8 (BL12XU) [31]. The synchrotron radiation from an undulator photon source was monochromated by a Si 111 double crystal monochromator. The polarization of the beam was then converted by a 0.5-mm-thick diamond phase plate to the circular or elliptical polarization. NaI scintillation detectors were mounted to monitor the air scattering along the vertical and horizontal axes, and the beam intensity and polarization parameters were determined from their outputs. The evaluated beam intensity on the sample was 1.1×10^{13} photons/s. The scattered photons from a Fe polycrystal sheet were monochromated by a 3×3 multianalyzer array of 2-m radius Si 555 bent crystals before being counted by a Si diode. Each analyzer had a mask that had a 85-mm-diam aperture, and thus the acceptance solid angle was 0.012 sr. The sample was magnetized in the 0.1-T field by an electromagnet. During the measurement, the magnetic field was flipped every 20 s to obtain the MCD spectra.

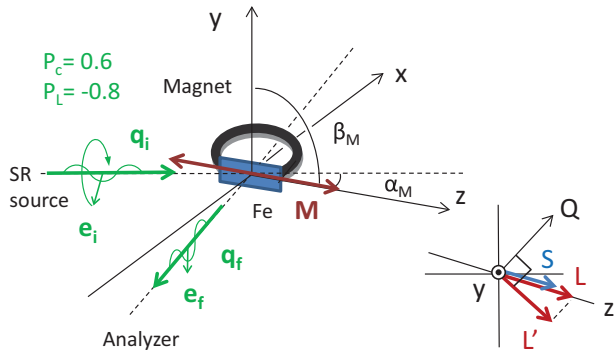


FIG. 1. (Color online) Geometry of the experiment: The scattering angle Θ is fixed at 90° . The z axis is parallel to magnetization vector \mathbf{M} while the y axis is parallel to $\hat{\mathbf{q}}_f \times \hat{\mathbf{q}}_i$. Therefore, \mathbf{L} and \mathbf{s} are parallel to the z axis while \mathbf{L}' is perpendicular to \mathbf{Q} and the y axis.

The magnetic scattering is a small contribution to the much stronger charge scattering. To extract such a weak signal, we can take advantage of the elliptical polarization. The right angle geometry ($\Theta = 90^\circ$) allows us not only to simplify the interpretation [Eqs. (7a)–(7d)] but also to make the experiment easier: One can minimize the charge scattering if we choose a suitable polarization. We chose the elliptical polarization of $P_L = -0.8$ and $P_C = 0.6$. Compared to the perfectly circular polarization case, we could enhance the magnetic effect by a factor of 3. The count rate was ~ 30 Hz at $P_C = 1$ while it was ~ 6 Hz at $P_C = 0.6$ at the L_{III} maximum. The data were accumulated for 4 days per an MCD spectrum, but the helicity of P_C was reversed every 24 h to confirm that the MCD sign flipped. Assuming that the inelastic behaviors are similar to the elastic one, we expect the OE1 scattering is dominant at $\alpha_M = 0^\circ$ while SM1 is dominant at -45 or 135° , and the total MCD signal becomes maximum at 90° once β_M is fixed at 90° (see Fig. 1). However, because of a geometrical constraint, we could not achieve such extreme conditions. The spectra were collected at three geometries of $(\alpha_M, \beta_M) = (15^\circ, 90^\circ)$, $(60^\circ, 90^\circ)$, and $(135^\circ, 75^\circ)$. An example of the experimental data is shown in Fig. 2. Weak but finite MCD signals flip the sign, depending on the polarity of P_L : This accords with a prediction of Eq. (7a).

The theoretical calculation was performed within a one-electron approximation. Equations (7a)–(7d) were evaluated using the local density matrices for the Fe $3d$ and $2p$ states in terms of the orbital and the spin magnetic quantum numbers m_l and m_s , the traces of which are the conventional, projected density of state. For the $3d$ states, the density matrix is calculated exploiting the *ab initio* band structure calculation, while for the $2p$ states, the $2p_{3/2}$ and $2p_{1/2}$ orbitals are assumed. As a first gross estimation, we adopted the diagonal approximation in which the $3d$ density matrix is diagonal for both orbitals and spins. It is known that Fe has an orbital magnetic moment of 4% to the spin magnetic moment, but this effect is not considered. In order to simulate the polycrystalline nature of the sample, we took the directional average for the $3d$ density matrix in terms of orbitals.

The experimental results are summarized in Fig. 3 along with theory. The theoretical curves are shifted downward. The

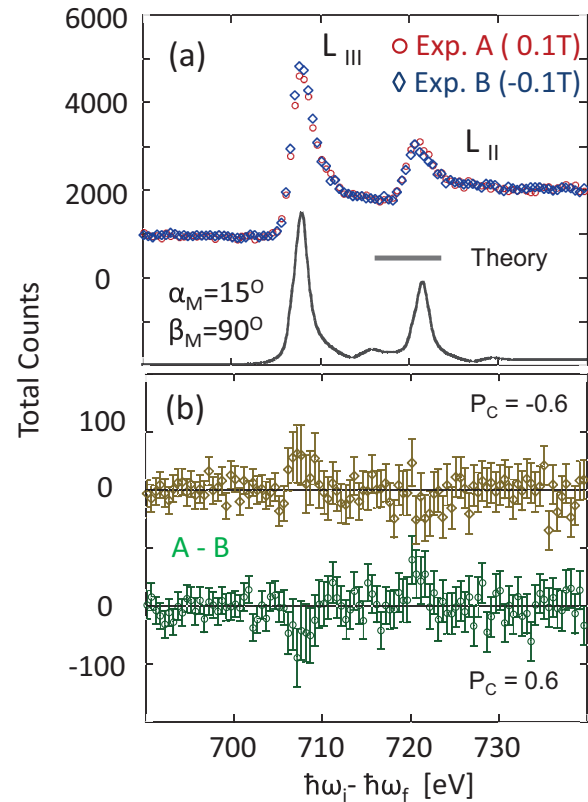


FIG. 2. (Color online) (a) XRS spectra measured under ± 0.1 T magnetic field and (b) their differences at $P_C = 0.6$ and -0.6 .

magnetic effect is about 2%, corresponding well to a prediction in Eq. (7a). An angular dependence is also recognizable. XRS-MCD at $\alpha_M = 15^\circ$ appears as XAS-MCD [8]. This represents a characteristic behavior of the spin scattering (C1-SM1), completely suppressed at $\mathbf{M} \perp \mathbf{q}_f$ or $\parallel \mathbf{q}_i$, i.e., $\alpha_M = 0^\circ$. The transition channels are totally occupied by $\Delta m_s = \pm 1$ transitions but they are canceled out by each other, leaving no amplitude: $N_{\tilde{n}} S_{\tilde{n}}^* \rightarrow 0$. On the other hand, the $N_{\tilde{n}} O_{\tilde{n}}^*$ channels make $\Delta m_l = \pm 1$ transitions and thus the orbital scattering (C1-OE1) becomes equivalent to XAS-MCD. This is sensibly understood once one realizes that $O_{\tilde{n}}$ can be transformed to $\langle f | i \mathbf{e}_{r\sigma} \cdot \mathbf{r} | i \rangle$, which has a shape similar to the transition matrix for XAS.

In contrast, XRS-MCD at $\alpha_M = 135^\circ$ appears as XAS. This is representative of a striking behavior of the orbital scattering (C1-OE1) at $\mathbf{M} \parallel \mathbf{Q}$: The transition vanishes because $N_{\tilde{n}}$ gives transitions with $\Delta m_l = 0$ while $O_{\tilde{n}}^*$ transitions with $\Delta m_l = \pm 1$, so their product becomes zero: $N_{\tilde{n}} O_{\tilde{n}}^* \rightarrow 0$. On the other hand, the spin scattering (C1-SM1) becomes equivalent to XAS because $N_{\tilde{n}} S_{\tilde{n}}^*$ involves only $\Delta m_s = 0$ transitions, resulting in a similar transition to the charge scattering (C1-C1), but the sign flips depending on the spin direction, namely, spin-dependent (spin-driven) XAS. Finally, XRS-MCD at $\alpha_M = 60^\circ$ is basically a sum of those: The features at L_{III} are suppressed while the features at L_{II} are enhanced.

We briefly comment here on the existence of a sum rule. Since the C1-OE1 transition channels are identical

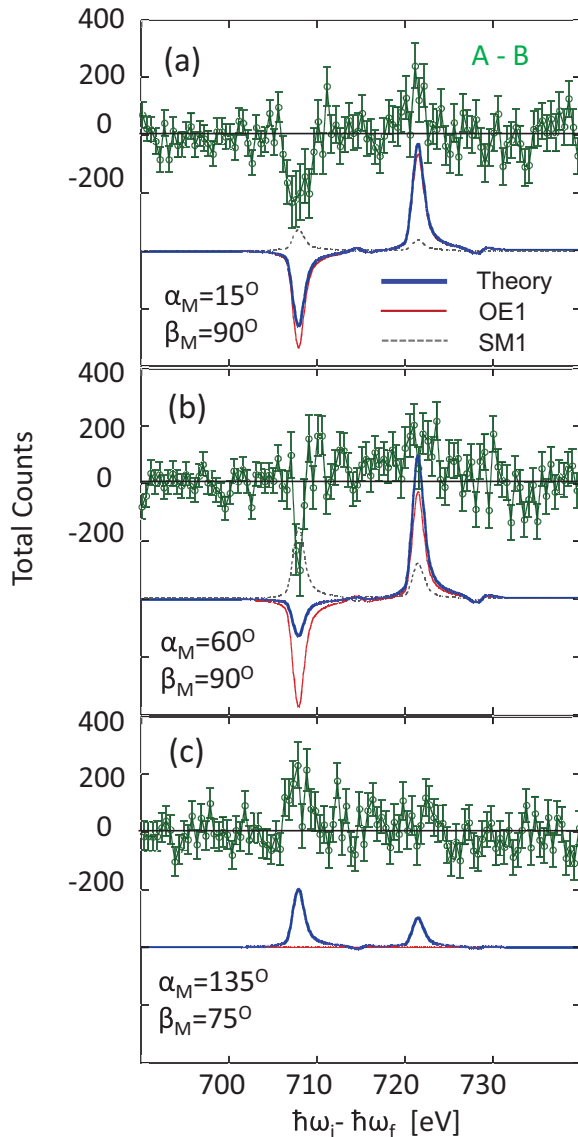


FIG. 3. (Color online) (a)–(c) XRS-MCD spectra at $(\alpha_M, \beta_M) = (15^\circ, 90^\circ)$, $(60^\circ, 90^\circ)$, and $(45^\circ, 75^\circ)$, along with theory. The thin solid line indicates the C1-OE1 transition while the dashed line indicates C1-SM1. The thick line is the sum of them. They are shifted downward for an easier comparison.

to those in XAS-MCD, the same sum rule should exist. Therefore, one may be able to apply the sum rule if the

MCD spectrum is measured in the exact $\mathbf{M} \parallel \mathbf{q}_i$ geometry in which the spin transition is suppressed. For such a quantitative analysis, it is essential to reveal the behavior of the C1-OM1 transition [Eq. (6d)] that is neglected in this study. Also, it is necessary to pay attention to the accuracy of the dipole approximation. Assuming $Q(r) = 0.87$ as the present condition, the main transition should be dipolar ($p \rightarrow d$), but higher-order transitions, mostly quadrupole ($p \rightarrow p$), can be contaminated as much as 15% to the XRS signals. Nonetheless, this effect would be very small because the spin polarization of the p state is much smaller than that of d . Another interesting possibility is to find a sum rule in $\mathbf{M} \parallel \mathbf{Q}$ geometry in which only the spin transition appears. Considering that only $\Delta m_l = 0$ transitions ($m_l = -1, 0, 1$) are allowed in this geometry, we believe that there would exist one of a different type, e.g., a partial sum rule among $|m_l| \leq 1$. Therefore, we might have information to resolve the orbital moments of $|m_l| = 2$ and of $|m_l| = 1$ once we measure the angular dependence of the XRS-MCD spectra or compare them with those of XAS-MCD. This possibility will be discussed elsewhere.

In summary, we have observed the MCD of nonresonant x-ray Raman scattering at $L_{II,III}$ edges in pure iron. The magnetic effect is $\sim 2\%$, which is in good agreement with magnetic scattering theory. The MCD spectra exhibit a significant angular dependence of the magnetization vector. We have also developed an effective theory to explain these behaviors. The XRS-MCD is equivalent to XAS-MCD when the magnetization vector \mathbf{M} is parallel to the incident wave vector \mathbf{q}_i once the scattering angle is fixed at 90° . In contrast, the XRS-MCD becomes spin-driven, spin-dependent XAS when \mathbf{M} is parallel to the scattering vector \mathbf{Q} . One of the ultimate goals of this study to apply this method to samples in an extreme condition, e.g., high pressure. Although it is too difficult to perform such an experiment at present in terms of the intensity, we believe that the problem will be overcome in the near future due to the improvement of the instrumentation.

We are grateful to Prof. M. Ito for useful discussions on magnetic diffraction. N.H. is deeply grateful to Prof. N. Sakai for sharing information and for fruitful discussions on magnetic Compton scattering. The experiment was performed under approvals of Japan Synchrotron Radiation Research Center (SPring-8 Proposal No. 2011B4250 and No. 2012A4253, 4254) and National Synchrotron Radiation Research Center, Taiwan (NSRRC Proposal No. 2011-2-105).

- [1] J. L. Erskine and E. A. Stern, *Phys. Rev. B* **12**, 5016 (1975).
- [2] G. Schütz, W. Wagner, W. Wilhelm, P. Kienle, R. Zeller, R. Frahm, and G. Materlik, *Phys. Rev. Lett.* **58**, 737 (1987).
- [3] C. T. Chen, F. Sette, Y. Ma, and S. Modesti, *Phys. Rev. B* **42**, 7262(R) (1990).
- [4] T. Koide, T. Shidara, H. Fukutani, K. Yamaguchi, A. Fujimori, and S. Kimura, *Phys. Rev. B* **44**, 4697(R) (1991).
- [5] P. Kuiper, B. G. Searle, P. Rudolf, L. H. Tjeng, and C. T. Chen, *Phys. Rev. Lett.* **70**, 1549 (1993).

- [6] B. T. Thole, P. Carra, F. Sette, and G. van der Laan, *Phys. Rev. Lett.* **68**, 1943 (1992).
- [7] P. Carra, B. T. Thole, M. Altarelli, and X. D. Wang, *Phys. Rev. Lett.* **70**, 694 (1993).
- [8] C. T. Chen, Y. U. Idzerda, H. J. Lin, N. V. Smith, G. Meigs, E. Chaban, G. H. Ho, E. Pellegrin, and F. Sette, *Phys. Rev. Lett.* **75**, 152 (1995).
- [9] K. Namikawa, M. Ando, T. Nakajima, and H. Kawata, *J. Phys. Soc. Jpn.* **54**, 4099 (1985).

- [10] S. P. Collins, D. Laundry, and A. J. Rollason, *Philos. Mag.* **65**, 37 (1992).
- [11] M. Ito, F. Itoh, Y. Tanaka, A. Koizumi, H. Sakurai, T. Ohta, K. Mori, A. Ochiai, and H. Kawata, *J. Phys. Soc. Jpn.* **64**, 2333 (1995).
- [12] N. Sakai and K. Ôno, *Phys. Rev. Lett.* **37**, 351 (1976).
- [13] N. Sakai, *J. Appl. Crystallogr.* **29**, 81 (1996).
- [14] M. H. Krisch, F. Sette, U. Bergmann, C. Masciovecchio, R. Verbeni, J. Goulon, W. Caliebe, and C. C. Kao, *Phys. Rev. B* **54**, R12673(R) (1996).
- [15] T. Iwazumi, K. Kobayashi, S. Kishimoto, T. Nakamura, S. Nanao, D. Ohsawa, R. Katano, and Y. Isozumi, *Phys. Rev. B* **56**, R14267(R) (1997).
- [16] A. Kotani and S. Shin, *Rev. Mod. Phys.* **73**, 203 (2001).
- [17] W. Schülke, U. Bonse, H. Nagasawa, A. Kaprolat, and A. Berthold, *Phys. Rev. B* **38**, 2112 (1988).
- [18] W. Schülke, *J. Phys.: Condens. Matter* **13**, 7557 (2001).
- [19] W. L. Mao, H. K. Mao, P. J. Eng, T. P. Trainor, M. Newville, C. C. Kao, D. L. Heinz, J. Shu, Y. Meng, and R. J. Hemley, *Science* **302**, 425 (2003).
- [20] Y. Q. Cai, H. K. Mao, P. C. Chow, J. S. Tse, Y. Ma, S. Patchkovskii, J. F. Shu, V. Struzhkin, R. J. Hemley, H. Ishii *et al.*, *Phys. Rev. Lett.* **94**, 025502 (2005).
- [21] W. L. Mao, H. K. Mao, Y. Meng, P. J. Eng, M. Y. Hu, P. Chow, Y. Q. Cai, J. Shu, and R. J. Hemley, *Science* **314**, 636 (2006).
- [22] J. F. Lin, H. Fukui, D. Prendergast, T. Okuchi, Y. Q. Cai, N. Hiraoka, C. S. Yoo, A. Trave, P. Eng, M. Y. Hu *et al.*, *Phys. Rev. B* **75**, 012201 (2007).
- [23] H. Fukui, M. Kanzaki, N. Hiraoka, and Y. Q. Cai, *Phys. Rev. B* **78**, 012203 (2008).
- [24] S. K. Lee, J. F. Lin, Y. Q. Cai, N. Hiraoka, P. J. Eng, T. Okuchi, H. K. Mao, Y. Meng, M. Y. Hu, P. Chow *et al.*, *Proc. Natl. Acad. Sci. USA* **105**, 7925 (2008).
- [25] Y. Meng, P. J. Eng, J. S. Tse, D. M. Shaw, M. Y. Hu, J. Shu, S. A. Gramsch, C. C. Kao, R. J. Hemley, and H. K. Mao, *Proc. Natl. Acad. Sci. USA* **105**, 11640 (2008).
- [26] M. Blume, *J. Appl. Phys.* **57**, 3615 (1985).
- [27] M. Blume and D. Gibbs, *Phys. Rev. B* **37**, 1779 (1988).
- [28] G. T. Trammell, *Phys. Rev.* **92**, 1387 (1953).
- [29] O. Steinsvoll, G. Shirane, R. Nathans, and M. Blume, *Phys. Rev.* **161**, 499 (1967).
- [30] See Supplemental Material at <http://link.aps.org/supplemental/10.1103/PhysRevB.91.241112> for Derivation of a simple formula for magnetic circular dichroism of nonresonant x-ray Raman scattering.
- [31] Y. Q. Cai, P. Chow, C. C. Chen, H. Ishii, K. L. Tsang, C. C. Kao, K. S. Liang, and C. T. Chen, in *Proceedings of the Eighth International Conference on Synchrotron Radiation Instrumentation*, edited by T. Warwick, J. Stöhr, H. A. Padmore, and J. Arthur, AIP Conf. Proc. No. 705 (AIP, Melville, NY, 2004), p. 340.